Neuron, Vol. 31, 487–495, August 16, 2001, Copyright ©2001 by Cell Press

Impaired Electrical Signaling Disrupts Gamma Frequency Oscillations in Connexin 36-Deficient Mice

Sheriar G. Hormuzdi,[1] Isabel Pais,[2] Fiona E.N. LeBeau,[2] Stephen K. Towers,[2] Andrei Rozov,[3] Eberhard H. Buhl,[2] Miles A. Whittington,[2] and Hannah Monyer[1,4]

[1] Department of Clinical Neurobiology
University Hospital of Neurology
Im Neuenheimer Feld 364
Heidelberg
Germany

[2] School of Biomedical Sciences
The Worsley Building
University of Leeds
Leeds LS2 9NQ
United Kingdom

[3] Max-Planck-Institut für medizinische Forschung
Jahnstrasse 29
69120 Heidelberg
Germany

Summary

Neural processing occurs in parallel in distant cortical areas even for simple perceptual tasks. Associated cognitive binding is believed to occur through the interareal synchronization of rhythmic activity in the γ (30–80 Hz) range. Such oscillations arise as an emergent property of the neuronal network and require conventional chemical neurotransmission. To test the potential role of gap junction-mediated electrical signaling in this network property, we generated mice lacking connexin 36, the major neuronal connexin. Here we show that the loss of this protein disrupts γ frequency network oscillations in vitro but leaves high frequency (150 Hz) rhythms, which may involve gap junctions between principal cells (Schmitz et al., 2001), unaffected. Thus, specific connexins differentially deployed throughout cortical networks are likely to regulate different functional aspects of neuronal information processing in the mature brain.

Introduction

Synchronous oscillatory activity in cortical brain regions has been proposed as a possible mechanism whereby distributed information is bound into a common representation (Singer, 1999; but see also Shadlen and Movshon, 1999). In particular, fast and ultrafast rhythms in hippocampal and neocortical areas underlie a range of cognitive processes, such as sensory perception, attention, and memory formation (Buzsaki et al., 1992; Cape et al., 2000; Csicsvari et al., 1999; Jones and Barth, 1999; Siapas and Wilson, 1998). In addition to the unequivocal importance of chemical neurotransmission in network activity, several recent studies have highlighted an important role for gap junction-mediated electrical coupling in the generation of synchronous population activity (Beierlein et al., 2000; Draguhn et al., 1998; Galarreta and Hestrin, 1999; Gibson et al., 1999; Tamas et al., 2000; Traub et al., 1999a). In support of this notion, computer simulations have indicated that electrical coupling may play a role not only in stabilizing synchronous population activity, but also in the generation of high frequency oscillations (~150 Hz) in the absence of chemical synapses (Draguhn et al., 1998; Traub et al., 1999a; White et al., 1998).

Expression of connexins, the protein constituents of gap junction channels, is more widespread during development, but electrical coupling has been also shown to occur in a number of brain structures in the adult brain (for review see Bennett, 1997). More recently, the presence of gap junctions and functional evidence of electrical coupling have been reported in GABAergic interneurons of the hippocampus and neocortex (Beierlein et al., 2000; Galarreta and Hestrin, 1999; Gibson et al., 1999; Tamas et al., 2000; Venance et al., 2000). Indeed, the recently cloned connexin 36 (Cx36; Condorelli et al., 1998; Sohl et al., 1998) was shown to be expressed at high levels in many regions of the adult rodent brain (Condorelli et al., 2000; Parenti et al., 2000). Furthermore, expression of Cx36 in the hippocampus corroborates the observation that gap-junction uncoupling agents abolish both ultrafast ripples as well as γ frequency network oscillations (Draguhn et al., 1998; Schmitz et al., 2001; Traub et al., 2000). These studies suggest that Cx36 may be an important component of the gap junctions responsible for the generation of synchronous oscillatory activity. Hence, we generated a mouse line which is devoid of Cx36 (Cx36 knockout) in order to assess the functional consequences of impaired electrical signaling on neuronal network activity.

Results

Generation of Cx36 Knockout Mice

In the Cx36 knockout mouse, a segment of the gene containing the second exon, which contributes all but 71 nucleotides (nt) of the Cx36 open reading frame (ORF; Condorelli et al., 1998; Sohl et al., 1998), was deleted (Figures 1A and 1B). The loss of Cx36 expression in P15 (postnatal day 15) Cx36 knockout offspring in contrast to wild-type (wt) siblings was documented by in situ hybridization (Figure 1C). Cx36 knockout mice appear normal, are fertile, and do not show any obvious abnormalities in CNS structure, development, and neuronal properties (data not shown).

Ultrafast, Gap Junction-Dependent Oscillations in Cx36 Knockout and Wild-Type Mice

To assess the consequences of the loss of Cx36 on neuronal network activity, we employed hippocampal slice preparations and studied ultrafast (100–200 Hz) population oscillations which are generated in the absence of chemical neurotransmission and are suggested to be an emergent property of the electrically coupled pyramidal cell network (Draguhn et al., 1998; Schmitz

[4] Correspondence: monyer@urz.uni-hd.de

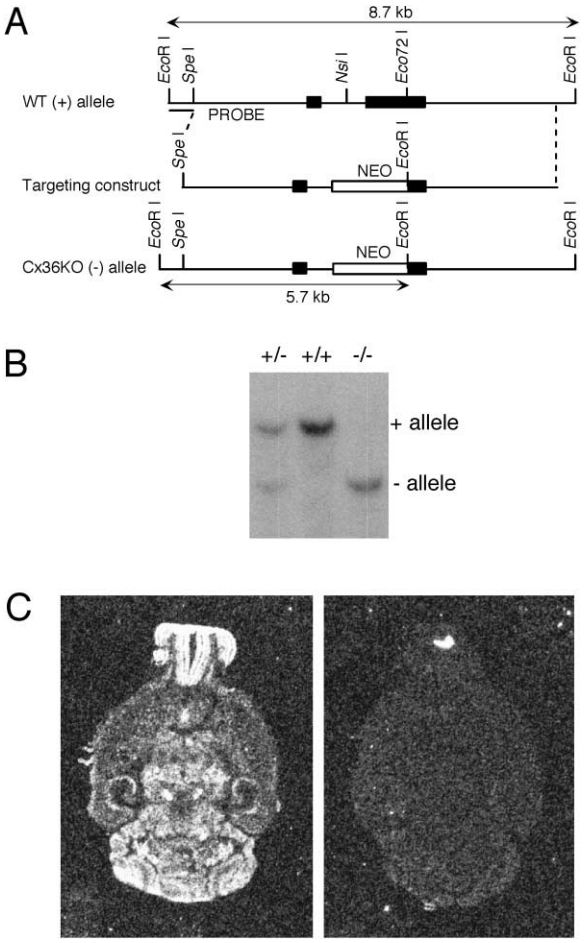

Figure 1. Disruption of the Connexin36 Gene

(A) The structure of the Cx36 gene within the wild-type allele, the Cx36 knockout allele, and the targeting construct are illustrated. Locations of the two exons (filled-in boxes) comprising the cDNA, and of the *neomycin* fragment (NEO) in the disrupted allele and targeting construct, along with relevant restriction endonuclease sites within the 8.7 kb EcoRI fragment derived from the locus are also indicated. Dashed lines indicate the ends of the targeting construct as they correspond to the wild-type sequence.

(B) A representative Southern blot demonstrating the procedure used to genotype mice is shown. The fragment indicated in (A) was used to probe EcoRI-restricted DNA from each of the three genotypes. The size and origins of the two fragments thus obtained are shown in (A) as arrows.

(C) X-ray autoradiography showing Cx36 expression in horizontal brain sections of P15 wild-type (left) and Cx36 knockout (right) siblings demonstrating the lack of expression in the knockout.

et al., 2001). In the presence of Ca^{2+}-free medium, extracellular field potential recordings in the pyramidal cell layer of the CA3 area of wild-type mouse hippocampi revealed characteristic bursts of high-frequency "ripples" (Figure 2A), which were reversibly abolished by the gap junctional uncoupling agent octanol (0.5–1 mM; $n = 5$). Likewise, slices of Cx36 knockout mice also exhibited ripple-like neuronal population discharges which were sensitive to octanol (Figure 2B; $n = 5$). These data therefore provide evidence for maintained ripple activity in networks of mutant hippocampi, irrespective of the loss of a major neuronal connexin.

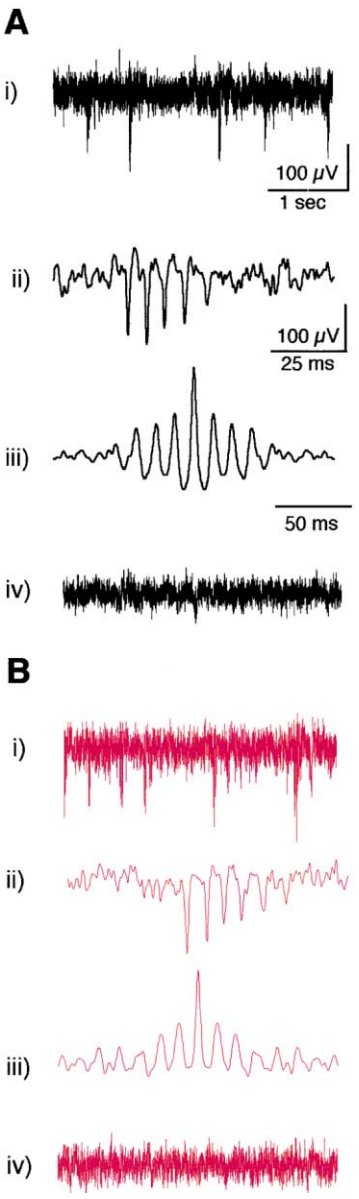

Figure 2. Effect of Cx36 Deletion on Hippocampal Ultrafast Population Activity

Data from wild-type and Cx36 knockout animals are shown in black and red, respectively. (A, i) Extracellular recording of fast spontaneous hippocampal ripples in the hippocampal CA3 area with individual burst of ripples (A, ii) and corresponding autocorrelation (A, iii) shown underneath. (B, i–iii) Bursts of ultrafast population oscillations were also evident in all slices of Cx36-deficient mice with no obvious changes in their overall appearance, frequency, and/or rhythmicity. (A, iv and B, iv) Bottom traces in each group reveal that spontaneous ripple activity in both wild-type and knockout mouse was abolished by superfusion with 1 mM of the gap junction uncoupling agent octanol.

Gamma Frequency Oscillations in Cx36 Knockout and Wild-Type Mice

Prompted by the predominant expression of Cx36 in hippocampal GABAergic interneurons (Venance et al., 2000), we proceeded to study pharmacologically induced γ frequency network oscillations, which depend

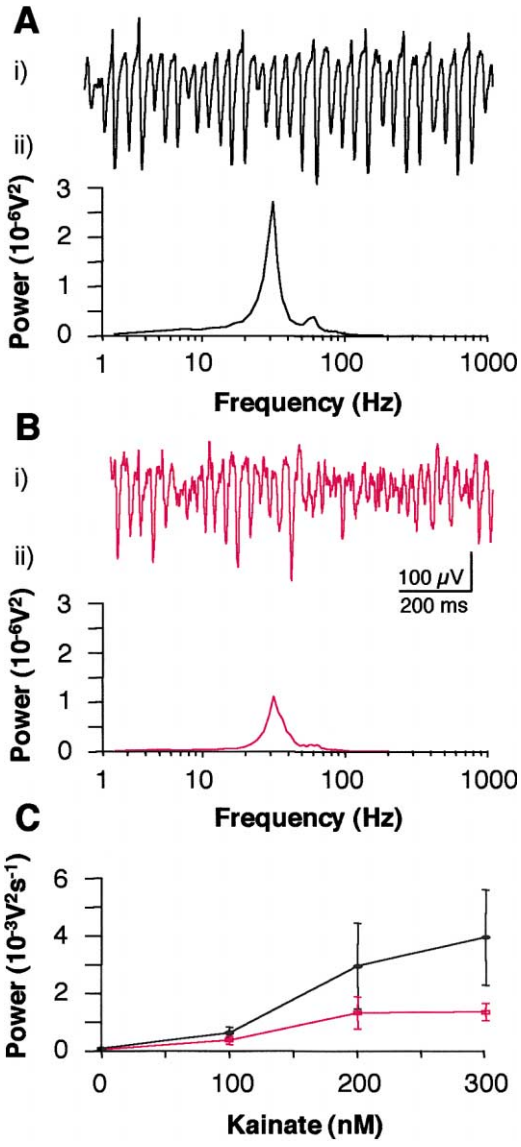

Figure 3. Effects of Cx36 Deletion on Hippocampal Population Gamma Activity Induced by Kainate

(A) In wild-type slices, superfusion with nanomolar concentrations of kainate (<400 nM) resulted in the appearance of persistent γ frequency network oscillations. The traces show an extracellular field recording taken in stratum radiatum of the CA3 area (A, i) and the corresponding power spectrum with a distinct peak in the γ frequency range underneath (A, ii). Sample trace of kainate-induced γ oscillatory activity in the CA3 area of a knockout mouse hippocampus (B, i) and corresponding power spectrum (B, ii). (C) Summary data showing the agonist concentration/spectral power (15–60 Hz) relationship of kainate-induced γ frequency oscillations in wild-type and Cx36 knockout mouse slices. Error bars denote SEM.

on both synaptic inhibition and gap junctional coupling (Traub et al., 2000). In slices of wild-type mice, nanomolar concentrations of kainate (Figure 3A; n = 8 slices from 5 animals) evoked the typical pattern of γ frequency population activity, which is both sensitive to bicuculline and to the gap junction blockers (data not shown; Fisahn et al., 1998; Traub et al., 2000). Although two-site recordings showed that intra-areal synchrony and peak frequency (wild-type: 33 ± 1 Hz, n = 5; knockout: 30 ± 1 Hz; n = 5) remained unaffected, it was apparent that the same concentrations of agonist consistently yielded lower amplitude oscillatory activity in Cx36 knockout slices (Figure 3B). Thus, more kainate was required to elicit a threshold response, and concentrations which were maximally effective in wild-type slices evoked significantly weaker oscillations in Cx36 knockout slices ($P < 0.05$, 2-way analysis of variance).

As it is conceivable that these results are to some extent model dependent, we employed another pharmacological paradigm, using a cholinergic agonist, carbachol, which is also known to evoke persistent oscillatory γ band activity (Fisahn et al., 1998). Quantification of the relationship between agonist concentration and spectral power yielded near-identical results to kainate-induced oscillations (Figures 4A–4C). Throughout the concentration range used (5–20 μM), larger oscillations were seen in slices from wild-type compared with Cx36 knockout mice (Figures 4A–4C; wild-type, n = 8 slices from 7 animals; knockout, n = 8 slices from 7 animals; $p < 0.05$).

In the networks producing γ activity described above, extracellular population activity is due to the reciprocal influence of pyramidal neurons *and* interneurons on a macroscopic scale within the slice (Fisahn et al., 1998). We therefore continued to investigate the activity of these cells with intracellular recordings from both major neuronal subtypes in oscillating slices in the presence of 200 nM kainate (Figure 5). At depolarized membrane potentials (−30 mV), pyramidal cells in the CA3 area of both wild-type and Cx36 knockout tissue revealed rhythmic membrane hyperpolarizations (Figure 5A), which, in view of their typical voltage dependence and bicuculline sensitivity, are likely to correspond to IPSPs. While inhibitory events in control cells exhibited uniformity and regularity (Figure 5A, i), those in Cx36-deficient slices appeared to be clearly disrupted in both amplitude and rhythmicity (Figure 5A, ii). Likewise, recordings from depolarized interneurons (−30 mV) in stratum pyramidale (n = 8) showed the same reduction in amplitude and variability of inhibitory inputs onto interneurons as seen for inhibitory inputs onto pyramidal cells (Figure 5B, i and ii). Analysis of intervals between temporally adjacent IPSPs showed a disruption in the timing of IPSPs in both pyramidal neurons (Figure 5A, iii) and interneurons (Figure 5B, iii). There was an increase in the incidence of longer periods between IPSPs, suggesting a more erratic pattern of period-by-period recruitment of interneuron firing during the oscillation. No significant difference in IPSP amplitudes was seen in interneurons ($P > 0.05$), despite a reduction in the median values (wild-type 3.8 mV, IQR 2.8–6.6; Cx36 knockout 3.0 mV, IQR 1.5–5.9). However, observed decreases in median IPSP amplitude in pyramidal cells did reach significance ($P < 0.05$; wild-type 5.7 mV, IQR 3.4–9.1; Cx36 knockout 4.4 mV, IQR 2.2–6.5). The pattern of interneuron EPSP (measured at −70 mV membrane potential) was also disrupted. Median EPSP amplitudes onto interneurons were significantly greater in the Cx36 knockout tissue than in the tissue from control, wild-type animals (wild-type 6.1 mV, IQR 4.2–12.5; Cx36 knockout 10.1 mV, IQR 6.0–19.5; $P < 0.01$).

Averaged power spectra of IPSP train recordings from

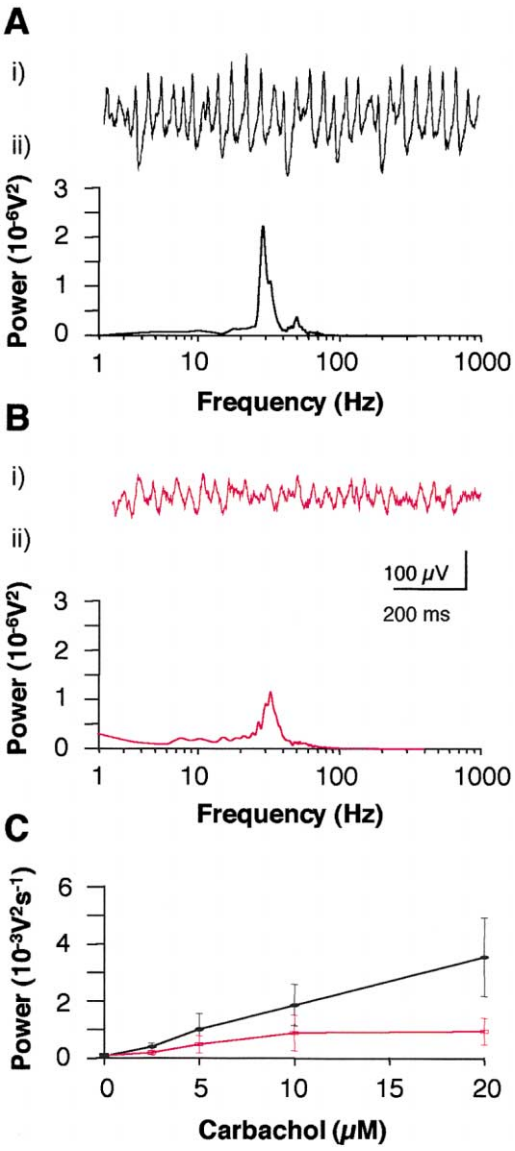

Figure 4. Effects of Cx36 Deletion on Hippocampal Population Gamma Activity Induced by Carbachol

(A) In wild-type slices, superfusion with carbachol (5– 20 μM) resulted in the appearance of persistent γ frequency network oscillations. The traces show an extracellular field recording taken in stratum radiatum of the CA3 area (carbachol concentration 20 μM) (A, i) and the corresponding power spectrum with a distinct peak in the γ frequency range underneath (A, ii). Sample trace of carbachol-induced (20 μM) γ oscillatory activity in the CA3 area of a knockout mouse hippocampus (B, i) and corresponding power spectrum (B, ii). (C) Summary data showing the agonist concentration/spectral power (15–60 Hz) relationship of carbachol-induced γ frequency oscillations in wild-type and Cx36 knockout mouse slices. Error bars denote SEM.

pyramidal cells revealed a marked reduction of oscillatory power in the γ frequency band (data not shown). Indeed, pooled and averaged autocorrelations of several recordings revealed a more prominent and consistent reduction in the amplitude of "side-peaks," indicating a large reduction in coherence of the inhibitory input onto pyramidal cells within the hippocampal network in Cx36 knockout mice (Figure 5A, iv and v). Oscillatory changes in interneurons could also be quantified as a dramatic loss of power in the γ frequency band (data not shown) and a marked reduction in network coherence demonstrated through autocorrelations (Figure 5B, iv and v). These alterations were indicative of an overall reduction in the rhythmicity of intracellular events.

Electrical Coupling between GABAergic Interneurons in Cx36 Knockout and Wild-Type Mice

The above data on γ oscillations demonstrate a change in oscillogenesis in macroscopic hippocampal networks where both interneurons and principal cells play a role on a scale comparable to the entire slice. We also show that nonsynaptic communication underlying ripple activity is unaffected in the Cx36 knockout mice (Figure 2). To further understand the mechanism behind the reduced oscillogenesis in Cx36 knockout mice, we looked at nonsynaptic communication between pairs of interneurons alone within the slice. Previous work in the neocortex has shown that gap junctional transmission between individual elements of the interneuron network results both in a net increase of the excitatory drive as well as an enhanced timing of action potential generation (Galarreta and Hestrin, 1999; Gibson et al., 1999; Tamas et al., 2000). Thus, if Cx36 were the prevalent gap junction forming protein in hippocampal interneurons, its loss may have resulted in the inability of these neurons to form functional electrical synapses. Such an alteration at the cellular level might underlie the observed changes in oscillatory network activity. To test this hypothesis, we performed dual whole-cell patch-clamp recordings of fast-spiking interneurons. As previously shown in the rat (Venance et al., 2000), electrical coupling could be detected in the majority of paired recordings from dentate gyrus basket cells in wild-type mice (Figure 6A). These cells were identified by their morphology, location, and fast-spiking firing pattern. Similar cells have been shown previously to contain parvalbumin (Venance et al., 2000). Reciprocal coupling was present in 12 of 13 pairs of such interneurons in wild-type mice ($n = 6$), but could not be detected in any of 17 pairs in Cx36 knockout mice ($n = 5$). We extended this analysis to pairs of fast-spiking GABAergic interneurons in CA3 stratum oriens and obtained similar results (data not shown). Electrical coupling was present in 5 out of 8 interneuron pairs in stratum oriens in wild-type mice ($n = 3$), but in none of 9 interneuron pairs in Cx36 knockout animals ($n = 3$). These results indicate that Cx36 is the molecular substrate of the electrical coupling reported in fast-spiking interneurons, and that DC coupling is completely abolished in this cell population in Cx36 knockout mice.

Electrical coupling between neurons is a source of both phasic and tonic excitation and is therefore likely to promote the generation of action potentials. Indeed, in pairs of electrically coupled dentate gyrus basket cells derived from wild-type mice, a subthreshold depolarizing current in one cell facilitated the generation of action potentials when concomitant firing was evoked in the second interneuron (4 out of 4 pairs, $n = 3$; Figure 6B). Conversely, no facilitation of action potential generation was observed in paired recordings of interneurons in Cx36 knockout mice (0 out of 6 pairs, $n = 2$; Figure 6B).

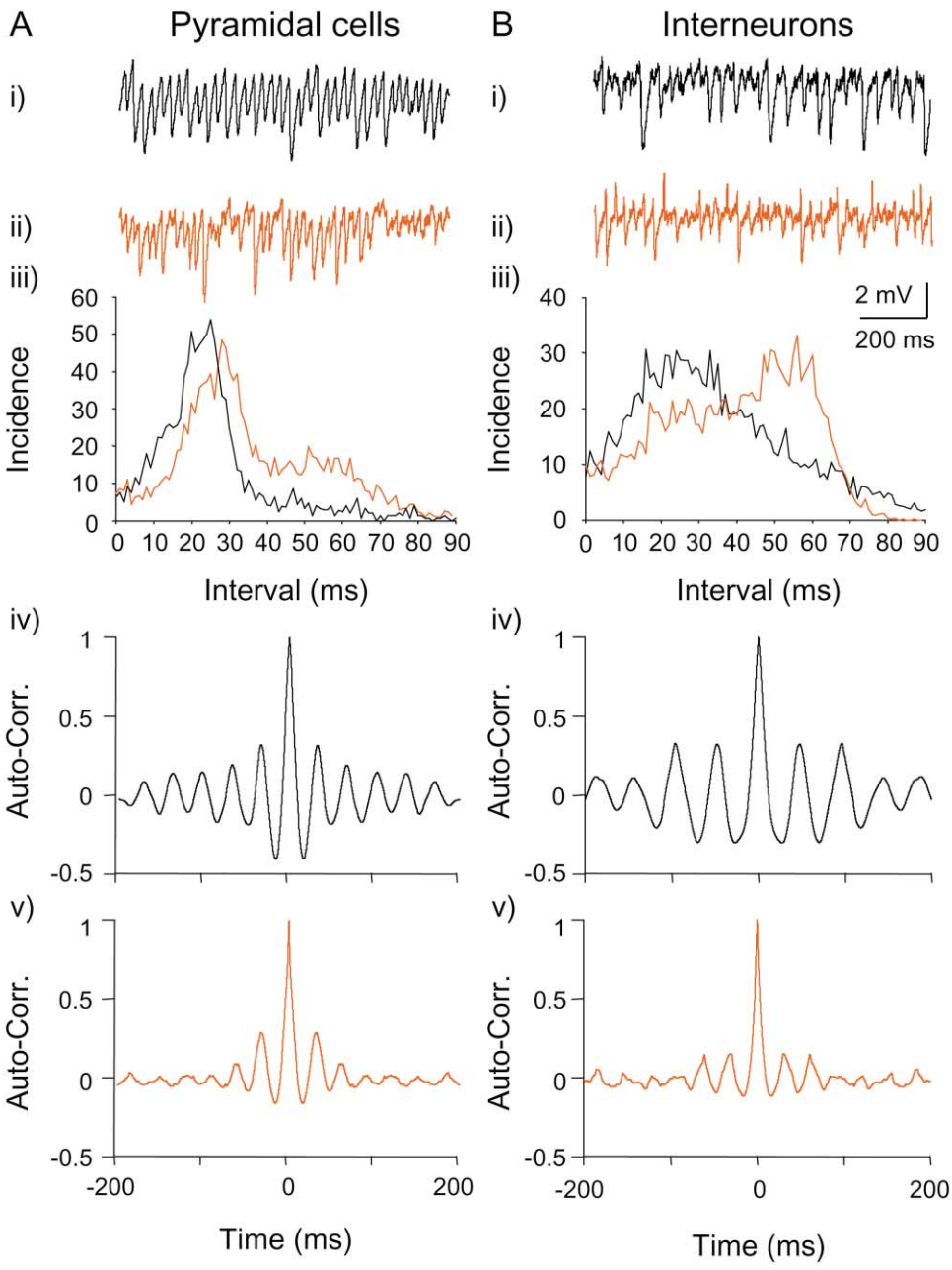

Figure 5. Effect of Cx36 Deletion on Intracellularly Recorded Oscillatory Activity of Hippocampal Neurons

Data from wild-type and Cx36 knockout animals are shown in black and red, respectively. (A, i) The top trace shows a current clamp recording of a wild-type CA3 pyramidal cell at a depolarized membrane potential, showing rhythmic IPSPs during kainate-induced γ frequency network activity. (A, ii) A corresponding sample trace of a CA3 pyramidal cell of a Cx36 knockout mouse is shown below. (A, iii) Pooled/averaged intersynaptic potential intervals from pyramidal cell recordings show γ band activity in both groups of cells, albeit with a greater incidence of longer interevent intervals in Cx36-deficient slices. Averaged autocorrelations from wild-type (A, iv) and Cx36 knockout mice (A, v) show a marked decrement in the amplitude of side peaks in Cx36 knockout mice, suggesting disrupted rhythmicity. (B, i) The top trace depicts a current clamp recording of a fast-spiking interneuron in the CA3 area of a wild-type mouse. (B, ii) Note the more erratic nature of IPSP amplitudes and intervals which are evident in an interneuron recording of a Cx36 knockout mouse. (B, iii) Pooled intersynaptic intervals from interneuron recordings in wild-type slices reveal a prominent peak in the γ frequency band, whereas the corresponding trace of the knockout mouse group has a broader distribution of intervals and a greater number of longer intervals reflecting the more erratic recruitment of interneurons on any given γ period. (B, iv) Averaged autocorrelations reveal a rhythmic γ frequency activity pattern in interneurons of wild-type mice, whereas the corresponding sample data of fast-spiking cells in knockout mouse tissue (B, v) were indicative of more irregular oscillations.

Postnatal Expression of Cx36 in Murine Brain

To better correlate the functional data with expression of Cx36 in the hippocampus, we performed an in situ hybridization study on postnatal brain obtained from wild-type mice. Whereas Cx36 mRNA was high in the olfactory bulb at all ages (Figure 7A), the abundance

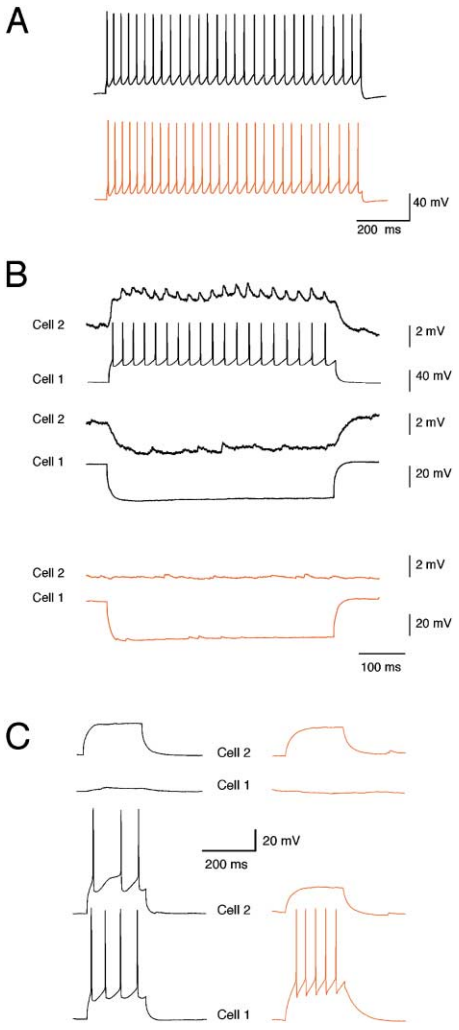

Figure 6. Loss of Electrical Coupling in Dentate Gyrus Fast-Spiking Interneurons

Sample traces (wild-type = black, Cx36 knockout = red) are shown in all instances. (A) Action potential firing pattern of a typical fast-spiking interneuron from the dentate gyrus of wild-type and Cx36 knockout mice. (B) In wild-type mice, voltage responses in cell 1 following depolarizing (upper traces) or hyperpolarizing (lower traces) current injection were reflected in cell 2, albeit with a significantly reduced amplitude. Current injection in Cx36 knockout neurons failed to evoke any response in the second cell (only hyperpolarizing traces are shown). (C) Cell 2 of a pair of wild-type (left) and Cx36 knockout (right) neurons was injected with subthreshold current pulses (upper traces). Only in coupled neurons from wild-type mice did cell 2 respond with action potentials upon injection of a depolarizing current in cell 1 (lower traces). This was not observed in neurons derived from Cx36 knockout.

of Cx36 transcript declined in all other brain regions evaluated, including the hippocampus. Since electrophysiological recordings were performed in the CA3 region, the Cx36 expression was examined in greater detail by emulsion autoradiography in this area (Figures 7B and 7C). Whereas virtually all neurons in the CA3 region express Cx36 early in development (P1, P7), only individual cells still express Cx36 following postnatal day 21. These labeled neurons are located in stratum oriens and radiatum, and a few are present in stratum pyramidale. The disappearance of Cx36 from the majority of cells in the pyramidal cell layer, as well as the location of the remaining Cx36-positive cells, is indicative of the GABAergic nature of these neurons. Indeed, as verified by single-cell RT-PCR experiments in slices derived from P30 mice, a PCR product with Cx36-specific primers could be obtained in 4 out of 5 GABAergic interneurons, but in none of 10 pyramidal neurons (data not shown).

These studies do not preclude the possibility that low levels of Cx36 expression, not detectable by in situ hybridization or by single-cell RT-PCR, persist in adult pyramidal neurons. However, they strongly suggest that, in the hippocampus, Cx36 is expressed in both principal cells and interneurons early in postnatal development, but primarily in interneurons in the adult.

Discussion

The data presented above demonstrate that the deletion of Cx36, a major neuronal gap junction protein, leads to the loss of functional electrical synapses between hippocampal interneurons in slices from adult animals. Paired recordings of GABAergic interneurons demonstrated that in Cx36 knockout mice, there is no compensatory effect that counteracts the loss of the normally occurring electrical coupling. Furthermore, the data indicate that the previously described DC coupling between GABAergic interneurons can be attributed entirely to Cx36-containing gap junctions.

Within the mutually connected interneuronal network, such an impairment of electrical signaling is likely to have two functional consequences. First, it will reduce the net excitatory drive to individual neuronal elements within the network and, consequently, raise the threshold for oscillatory population activity. The ability of interneurons to "share" tonic drive (depolarization) via gap junctions would also reduce any heterogeneity of drives to individual interneurons within an oscillating network. Computer modeling has predicted that γ oscillations involving populations of interneurons are exquisitely sensitive to heterogeneity of driving forces, with increasing heterogeneity of interneuronal depolarizations rapidly resulting in a collapse of the oscillation (White et al., 1998). Second, any synchronizing function of electrical coupling potentials will be lost, diminishing the precision of action potential timing and resulting in an impairment of rhythmicity. The outcome of these two alterations is clearly reflected in the reduction of rhythmicity in the γ frequency band during oscillations induced in the entire network in slices from Cx36 knockout mice, suggesting that Cx36 is required for physiological expression of this activity.

In hippocampal slices from adult rodents, γ oscillations can occur transiently in interneuron networks in the absence, or near absence, of fast excitatory drive to interneurons (Whittington et al., 2001; Whittington et al., 1995). However, the majority of activity at γ frequencies is recorded from the hippocampus in vivo as an ongoing, persistent oscillation, often modulated at theta frequencies and associated with exploratory behavior (Bragin et al., 1995). In vitro models of this on-going, behaviorally correlated γ activity demonstrate a critical

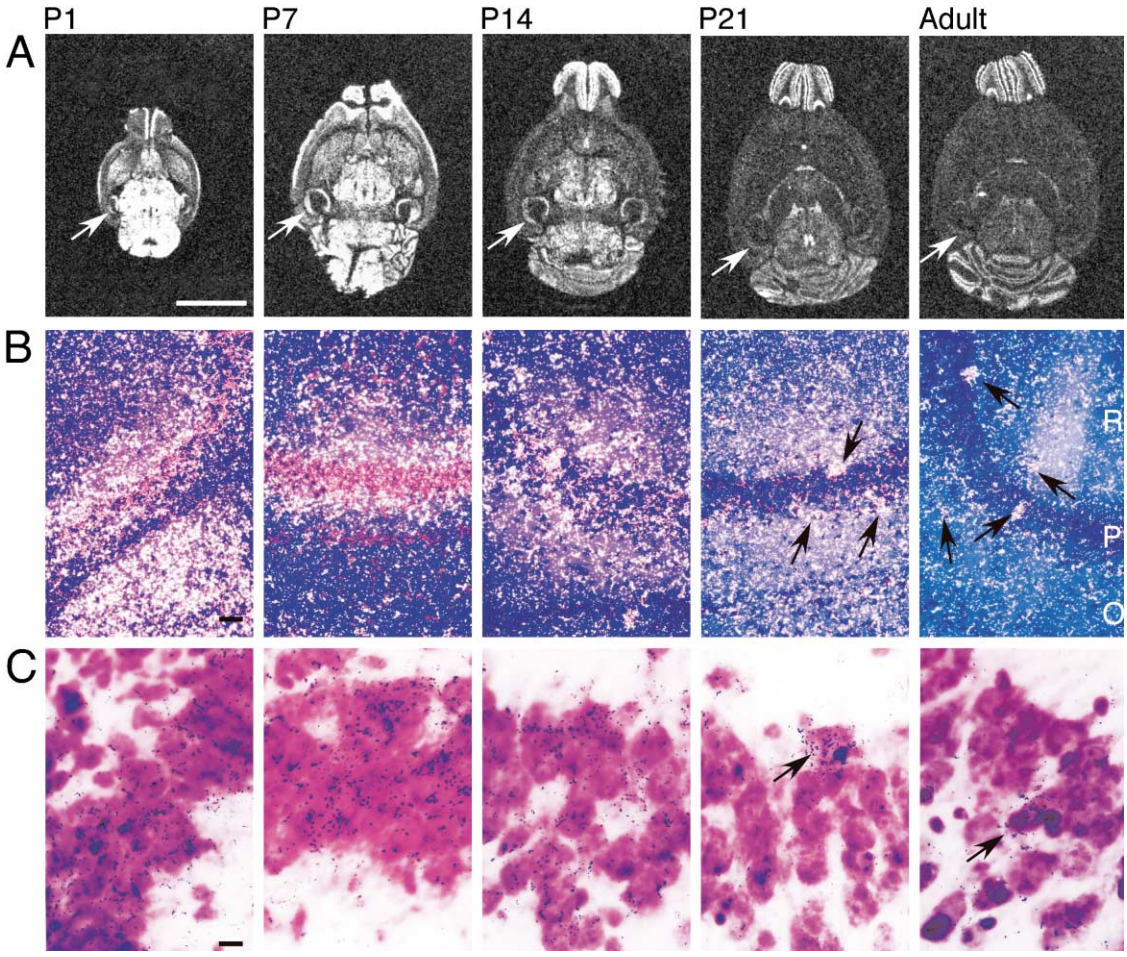

Figure 7. Postnatal Distribution of Cx36 mRNA

(A) X-ray autoradiography illustrating the distribution of transcripts encoding Cx36 in horizontal brain sections obtained from wild-type mice. Arrows point to the hippocampus in all the panels. Dark-field (B) and bright field (C) photomicrographs from emulsion autoradiography experiments highlighting the decrease in the expression of Cx36 in the CA3 pyramidal cell layer (P) during postnatal development. The orientation of the hippocampus is similar for all the panels in (B) and is indicated for the adult (O = stratum oriens, P = stratum pyramidale, R = stratum radiatum). Arrows indicate putative GABAergic interneurons in P21 and adult mice which contain Cx36 transcripts in abundance. (Scale bar: A = 4 mm; B = 50μm; C = 10μm.)

involvement of phasic excitatory drive to interneurons (Fisahn et al., 1998). The present observations demonstrated that this persistent oscillation was disrupted, though not abolished, by an apparent absence of functional gap junction-mediated communication within the interneuron network only. We suggest that phasic inhibitory synaptic inputs onto both principal cells and other interneurons were temporally disrupted as a consequence of the absence of nonsynaptic communication within the interneuron network. In contrast, nonsynaptic communication within the excitatory neuronal network, as measured using ultrafast population activity, was normal. These ultrafast oscillations were described by Draguhn et al. (1998) who showed that such activity was a population phenomenon accompanied by rapid coupling potentials in pyramidal neurons which could be blocked or enhanced by a range of agents affecting gap junctional activity. In addition, the gap junctions which could mediate this rhythm have been identified as occurring between axons of principal cells approximately 100 μm from the soma (Schmitz et al., 2001). Thus, despite the ability of the network to precisely, nonsynaptically time principal cell outputs onto interneurons, removal of this putative mechanism in the interneuron network is sufficient to disrupt oscillations in the macroscopic network. In fact, expression analysis of Cx36 in the adult mouse, as demonstrated both by in situ hybridization and by single-cell RT-PCR, is in concordance with the electrophysiological data indicating the functional importance of this protein for GABAergic interneurons, but not for principal cells. The higher and more widespread expression of Cx36 at embryonic (Gulisano et al., 2000) and early postnatal developmental stages (Figure 7) implies that Cx36 may serve additional functions in the young brain (for a review of a possible role of gap junctions in the developing brain, see Kandler and Katz, 1995).

With discrete, spatially separate oscillating areas, or large spatially distributed oscillating networks, the longer-range synchronization has been suggested to be

mediated by excitatory synaptic projections onto more distal interneurons (Karbowski and Kopell, 2000; Traub et al., 1999b). The two models of γ oscillations used in the present study can be most accurately considered as spatially distributed network generators. Thus, disruption of local rhythmicity and synchrony would be reflected across the entire oscillating region as indicated in reduced cross correlations with paired extracellular recordings with >200 μm separation (data not shown). Acute, global disruption of gap junctional activity with carbenoxolone or octanol completely abolishes γ oscillations in the model used here (e.g., see Traub et al., 2000). Partial disruption of gap junctional transmission, with carbenoxolone, produces activity where the amplitude and coherence of the field oscillation are maintained, but concentration-dependent increases in the incidence and duration of periods of quiescence are observed (I.P., F. L., and E.B., unpublished observations). This type of "all-or-none" effect of global gap junctional blockade did not represent the deficits seen in tissue from Cx36-deficient animals. This comparison suggests that interneuron-selective disruption of gap junctional activity has a more subtle, specific effect of γ rhythmogenesis, with the oscillation maintained qualitatively, but temporal relationships within the oscillating network being disrupted.

In summary, the present data demonstrate that Cx36 knockout disrupts nonsynaptic interneuronal communication in interneurons but *not* pyramidal cells. The lack of Cx36 in interneurons leads to a disruption of oscillogenesis in macroscopic networks in models of persistent γ oscillations. This study provides genetic evidence for the role of a specific gap junction forming protein in mediating synchronous neuronal activity in large-scale hippocampal networks.

Experimental Procedures

Generation of Cx36 Knockout Mice

All manipulations were performed within an ~8.7 kb EcoR I genomic fragment containing the two exons encoding the Cx36 cDNA. The targeting construct, cloned in pBluescript (Stratagene USA), began at the SpeI site and ended ~450 nt 5′ to the 3′ end of the alleles (ends are indicated as dashed lines). This construct was altered as described below. A *neomycin* cassette (provided generously by Dr. A.F. Stewart), wherein expression of *neo* was driven by the SV 40 early enhancer/promoter, flanked immediately by FRT elements and by a single *loxP* sequence at the 3′ end was introduced into the NsiI site. Subsequent manipulations replaced the Eco72I site, which is located 163 nt past the termination codon of the Cx36 gene, with an additional *loxP* sequence and an EcoRI restriction endonuclease sequence at its 3′ end. The NsiI-Eco72I fragment containing the entire second exon, which comprises all but 71 nt of the open reading frame, was deleted in *E. coli* by homologous recombination between the two *loxP* sequences (Zhang et al., 1998). Homologous recombination in embryonic stem (ES) cells and subsequent generation of Cx36 knockout mice was done in the usual manner (Bronson and Smithies, 1994; Capecchi, 1989). Southern blot analysis of EcoRI-restricted DNA was done to screen ES cells and genotype mice. For this purpose, the fragment between the 5′ EcoRI and SpeI sites (see figure) was used to probe blots. In this manner, the 8.7 kb and 5.7 kb fragments, derived from the wild-type and mutant alleles, respectively, could be distinguished.

In Situ Hybridization

In situ hybridization experiments (Figure 7) were performed on mice of different stages of early postnatal development, and on the adult (P60–P90). The experiments were performed as previously described (Wisden and Morris, 1994). Briefly, the antisense oligonucleotides 5′-GGTGGTCTCTGTGTTCTGCAGCA CCCCATTGACCAT GGC-3′ and 5′- CTGGGCTCCCCGGACAGCC AGTTTGATCTTCCGC CAT-3′, corresponding to nt 442–480 and 828–864, respectively, of the Cx36 ORF were 3′ end labeled using terminal deoxynucleotidyl transferase and (α)-^{35}S dATP. Similar results were obtained with the two oligonucleotides. Sections were hybridized overnight at 42°C in 50% formamide, 4× SSC (0.6 M NaCl, 0.06 M sodium citrate), 10% dextran sulfate with 1 pg/μl labeled oligonucleotide. The sections were washed in 1× SSC at 60°C for 20 min and exposed to Kodak XAR-5 film for 21 days. For cellular resolution, sections were dipped in Kodak NTB3 emulsion and exposed at 4°C for 8 weeks. After development, sections were counterstained with 0.1% thionin and viewed with a Zeiss Axioplan microscope.

Single-Cell RT-PCR

Single-cell RT-PCR experiments were performed as described earlier (Venance et al., 2000) on slices obtained from P30 mice. Cytosolic material harvested from individual pyramidal cells and interneurons, identified by their shape, location, and firing pattern, was subjected to two consecutive amplification cycles utilizing Cx36-specific primers. The 277 bp fragment so amplified was identified by agarose gel electrophoresis.

Electrophysiology

Slice preparation, artificial cerebrospinal fluid (ACSF) composition, recordings with sharp microelectrode,s and analysis techniques were as described (Fisahn et al., 1998). Brain slices were prepared from 3- to 6-month-old mice. All drugs were dissolved in ACSF and bath-applied. For preparation of Ca^{2+}-free medium, Ca^{2+} in the ACSF was replaced by 2 mM Mg^{2+}. Dose response curves were obtained by placing wild-type and Cx36 knockout mouse slices side-by-side into the slice chamber and by increasing agonist concentration in regular increments. Spectral power was integrated across the γ frequency band (20–80 Hz) and averaged for each concentration and experimental group. Statistical comparisons were made with a Bonferroni t test. Pyramidal neurons and interneurons were impaled with sharp electrodes for synaptic analysis and classified electrophysiologically using the following parameters: action potential width at half-height, accommodation pattern, early AHP profile, and E/IPSP kinetics. Synaptic potential analysis was performed using "MiniAnalysis" (Synaptosoft) with data from >1000 E/IPSPs taken from each cell from each animal (n = 4 cells per genotype). Autocorrelations of sample traces were normalized for time to account for differences in the oscillation frequency of individual recordings, thus resulting in an alignment of side peaks. Normalized autocorrelations were then averaged, thus reflecting the degree of rhythmicity within a given group.

Paired recordings of fast-spiking hippocampal interneurons were obtained using the whole-cell patch-clamp technique as previously described for electrically coupled interneurons in the dentate gyrus (Venance et al., 2000). All brain slices were prepared from P13–P22 mice, and almost all studies were conducted on wild-type and Cx36 knockout littermates, although a few wild-type mice from our in-house animal facility were used in some instances. In order to identify coupled cell pairs, first a neuron with the appropriate appearance and action potential firing pattern was identified. Then another neuron with the same properties and within a distance of 50 μm from the first one was located and patched. Coupling was then determined as previously described (Venance et al., 2000).

Acknowledgments

We thank F. Zimmerman and U. Amtmann for technical assistance, Dr. A.F. Stewart for providing the *neomycin* cassette, Dr. P. Seeburg for a critical reading of the manuscript and for suggestions, Dr. D.L. Paul for sharing results, and Dr. A. Caputi for help with the manuscript. Special thanks go to Dr. R. Traub for stimulating discussions and helpful suggestions. This work was supported in part by grants of the Medical Research Council to E.H.B. and M.A.W., the Schilling Foundation and the DFG (SFB 488) to H.M.

Received April 9, 2001; revised July 23, 2001.

References

Beierlein, M., Gibson, J.R., and Connors, B.W. (2000). A network of electrically coupled interneurons drives synchronized inhibition in neocortex. Nat. Neurosci. *3*, 904–910.

Bennett, M.V. (1997). Gap junctions as electrical synapses. J. Neurocytol. *26*, 349–366.

Bragin, A., Jando, G., Nadasdy, Z., Hetke, J., Wise, K., and Buzsaki, G. (1995). Gamma (40–100 Hz) oscillation in the hippocampus of the behaving rat. J. Neurosci. *15*, 47–60.

Bronson, S.K., and Smithies, O. (1994). Altering mice by homologous recombination using embryonic stem cells. J. Biol. Chem. *269*, 27155–27158.

Buzsaki, G., Horvath, Z., Urioste, R., Hetke, J., and Wise, K. (1992). High-frequency network oscillation in the hippocampus. Science *256*, 1025–1027.

Cape, E.G., Manns, I.D., Alonso, A., Beaudet, A., and Jones, B.E. (2000). Neurotensin-induced bursting of cholinergic basal forebrain neurons promotes gamma and theta cortical activity together with waking and paradoxical sleep. J. Neurosci. *20*, 8452–8461.

Capecchi, M.R. (1989). The new mouse genetics: altering the genome by gene targeting. Trends Genet. *5*, 70–76.

Condorelli, D.F., Parenti, R., Spinella, F., Trovato Salinaro, A., Belluardo, N., Cardile, V., and Cicirata, F. (1998). Cloning of a new gap junction gene (Cx36) highly expressed in mammalian brain neurons. Eur. J. Neurosci. *10*, 1202–1208.

Condorelli, D.F., Belluardo, N., Trovato-Salinaro, A., and Mudo, G. (2000). Expression of Cx36 in mammalian neurons. Brain Res. Brain Res. Rev. *32*, 72–85.

Csicsvari, J., Hirase, H., Czurko, A., Mamiya, A., and Buzsaki, G. (1999). Fast network oscillations in the hippocampal CA1 region of the behaving rat. J. Neurosci. *19*, RC20.

Draguhn, A., Traub, R.D., Schmitz, D., and Jefferys, J.G. (1998). Electrical coupling underlies high-frequency oscillations in the hippocampus in vitro. Nature *394*, 189–192.

Fisahn, A., Pike, F.G., Buhl, E.H., and Paulsen, O. (1998). Cholinergic induction of network oscillations at 40 Hz in the hippocampus in vitro. Nature *394*, 186–189.

Galarreta, M., and Hestrin, S. (1999). A network of fast-spiking cells in the neocortex connected by electrical synapses. Nature *402*, 72–75.

Gibson, J.R., Beierlein, M., and Connors, B.W. (1999). Two networks of electrically coupled inhibitory neurons in neocortex. Nature *402*, 75–79.

Gulisano, M., Parenti, R., Spinella, F., and Cicirata, F. (2000). Cx36 is dynamically expressed during early development of mouse brain and nervous system. Neuroreport *11*, 3823–3828.

Jones, M.S., and Barth, D.S. (1999). Spatiotemporal organization of fast (>200 Hz) electrical oscillations in rat Vibrissa/Barrel cortex. J. Neurophysiol. *82*, 1599–1609.

Kandler, K., and Katz, L.C. (1995). Neuronal coupling and uncoupling in the developing nervous system. Curr. Opin. Neurobiol. *5*, 98–105.

Karbowski, J., and Kopell, N. (2000). Multispikes and synchronization in a large neural network with temporal delays. Neural Comput. *12*, 1573–1606.

Parenti, R., Gulisano, M., Zappala, A., and Cicirata, F. (2000). Expression of connexin36 mRNA in adult rodent brain. Neuroreport *11*, 1497–1502.

Schmitz, D., Schuchmann, S., Fisahn, A., Draguhn, A., Buhl, E.H., Petrash-Parvez, R.E., Dermietzel, R., Heinemann, U., and Traub, R.D. (2001). Axo-axonal coupling: a new mechanism for ultrafast neuronal communication. Neuron, in press.

Shadlen, M.N., and Movshon, J.A. (1999). Synchrony unbound: a critical evaluation of the temporal binding hypothesis. Neuron *24*, 67–77.

Siapas, A.G., and Wilson, M.A. (1998). Coordinated interactions between hippocampal ripples and cortical spindles during slow-wave sleep. Neuron *21*, 1123–1128.

Singer, W. (1999). Time as coding space? Curr. Opin. Neurobiol. *9*, 189–194.

Sohl, G., Degen, J., Teubner, B., and Willecke, K. (1998). The murine gap junction gene connexin36 is highly expressed in mouse retina and regulated during brain development. FEBS Lett. *428*, 27–31.

Tamas, G., Buhl, E.H., Lorincz, A., and Somogyi, P. (2000). Proximally targeted GABAergic synapses and gap junctions synchronize cortical interneurons. Nat. Neurosci. *3*, 366–371.

Traub, R.D., Schmitz, D., Jefferys, J.G., and Draguhn, A. (1999a). High-frequency population oscillations are predicted to occur in hippocampal pyramidal neuronal networks interconnected by axo-axonal gap junctions. Neurosci. *92*, 407–426.

Traub, R.D., Whittington, M.A., Buhl, E.H., Jefferys, J.G., and Faulkner, H.J. (1999b). On the mechanism of the gamma → beta frequency shift in neuronal oscillations induced in rat hippocampal slices by tetanic stimulation. J. Neurosci. *19*, 1088–1105.

Traub, R.D., Bibbig, A., Fisahn, A., Lebeau, F.E., Whittington, M.A., and Buhl, E.H. (2000). A model of gamma-frequency network oscillations induced in the rat CA3 region by carbachol in vitro. Eur. J. Neurosci. *12*, 4093–4106.

Venance, L., Rozov, A., Blatow, M., Burnashev, N., Feldmeyer, D., and Monyer, H. (2000). Connexin expression in electrically coupled postnatal rat brain neurons. Proc. Natl. Acad. Sci. USA *97*, 10260–10265.

White, J.A., Chow, C.C., Ritt, J., Soto-Trevino, C., and Kopell, N. (1998). Synchronization and oscillatory dynamics in heterogeneous, mutually inhibited neurons. J. Comput. Neurosci. *5*, 5–16.

Whittington, M.A., Traub, R.D., and Jefferys, J.G. (1995). Synchronized oscillations in interneuron networks driven by metabotropic glutamate receptor activation. Nature *373*, 612–615.

Whittington, M.A., Doheny, H.C., Traub, R.D., LeBeau, F.E., and Buhl, E.H. (2001). Differential expression of synaptic and nonsynaptic mechanisms underlying stimulus-induced gamma oscillations in vitro. J. Neurosci. *21*, 1727–1738.

Wisden, W., and Morris, B.J. (1994). *In situ* hybridization with synthetic oligonucleotide probes. In *In situ* hybridization protocols for the brain, W. Wisden and B.J. Morris, eds. (London: Academic Press), pp. 9–34.

Zhang, Y., Buchholz, F., Muyrers, J.P., and Stewart, A.F. (1998). A new logic for DNA engineering using recombination in Escherichia coli. Nat. Genet. *20*, 123–128.